Supporting Information

Interstellar Formation of the Elusive Phosphanyloxyphosphane (H_2POPH_2) and Phosphanylphosphinous Acid (H_2PPHOH) via Non-Equilibrium Chemistry – Precursors to the Phosphate Backbone of Nucleotides

Jia Wang,[1,2] Bing-Jian Sun,[3] Alexandre Bergantini,[1,2] Zesen Wang,[1,2] Andrew M. Turner,[1,2] Agnes H. H. Chang,[3*] Ralf I. Kaiser[1,2*]

[1] *W. M. Keck Research Laboratory in Astrochemistry, University of Hawaii at Manoa, Honolulu, Hawaii 96822, United States*

[2] *Department of Chemistry, University of Hawaii at Manoa, Honolulu, Hawaii 96822, United States*

[3] *Department of Chemistry, National Dong Hwa University, Shoufeng, Hualien 974, Taiwan*

[*]Corresponding Authors:

Agnes H. H. Chang, hhchang@gms.ndhu.edu.tw

Ralf I. Kaiser, ralfk@hawaii.edu

Methods

Experimental. All experiments were carried out in an ultrahigh vacuum chamber maintained at base pressures of a few 10^{-11} Torr using magnetically suspended turbomolecular pumps and an oil-free scroll pump.[1] Inside the main chamber, a polished silver substrate is mounted to a cold head to reach temperatures as low as 5 K. The cold head is connected to a closed cycle helium compressor and can be vertically adjusted via a bellows and rotated in the horizontal plane using a rotatable flange. The experimental procedures have been previously described in detail elsewhere.[2,3] Phosphine (PH_3, Sigma-Aldrich, 99.9995%), carbon dioxide (CO_2, Airgas, 99.999%), isotopically labeled carbon dioxide-^{13}C ($^{13}CO_2$, Sigma-Aldrich, 99 atom % ^{13}C) and carbon dioxide-$^{18}O_2$ ($C^{18}O_2$, Sigma-Aldrich, 95 atom % ^{18}O) were used in the experiments. Phosphine and carbon dioxide were premixed in a gas mixing chamber at a ratio of phosphine to carbon dioxide of 1:10. Once the substrate reached 5 K, the gas mixture was deposited onto the substrate via a glass capillary array at a pressure of 2×10^{-8} Torr. The ice thickness was determined to be 830 ± 50 nm using laser interferometry; the ratio of phosphine to carbon dioxide was determined to be 1:10 using the integrated infrared absorption areas along with absorption coefficients of the reactants.[3] After deposition, the ice mixtures were irradiated with 5 keV electrons, simulating secondary electrons generated by galactic cosmic rays (GCRs) as they pass through the interstellar ices within cold molecular clouds.[4] Infrared spectra of the ices were recorded in situ using a Fourier Transform Infrared (FTIR) spectrometer in the 6000–500 cm^{-1} range before, during, and after irradiation. The PH_3−CO_2 ice mixtures were processed with 5 keV electrons at nominal beam current of 100 nA for 60 minutes, corresponding to doses of 2.5 ± 0.4 eV per PH_3 molecule and 3.5 ± 0.6 eV per CO_2 molecule, as calculated using the CASINO software suite.[5] These doses simulate the energy input from secondary electrons generated by GCRs over timescales equivalent to molecular cloud lifetimes of up to $(8 \pm 2) \times 10^6$ years.[6] Utilizing the densities of PH_3 (0.90 g cm^{-3})[7,8] and CO_2 (0.98 g cm^{-3}),[9] the average penetration depth of electrons in PH_3−CO_2 ice was determined to be 360 ± 50 nm; 99% of the electron energy was deposited in the top 560 ± 50 nm of the ice—less than ice thickness (830 ± 50 nm)—preventing interactions between electrons and the substrate. After irradiation, the ice mixtures were subjected to temperature-programmed desorption (TPD), heating from 5 to 320 K at a rate of 1 K min^{-1}. During TPD, subliming molecules were photoionized in the gas phase using pulsed (30 Hz) vacuum ultraviolet (VUV) photons produced via two photon resonant four-wave mixing in a krypton/xenon

gas jet. The fundamental laser beams were generated via two tunable dye lasers and two Nd:YAG lasers. Detailed VUV photon generation parameters, including photon energies of 10.86, 9.60, 8.77, and 8.11 eV, are provided in Table S4. The VUV light was separated spatially via a biconvex lithium fluoride lens and passed through 2.0 ± 0.5 mm above the substrate to ionize the subliming compounds. A reflectron time-of-flight mass spectrometer (ReToF-MS) was used to detect the resulting ions; the ion signals were amplified, discriminated, and collected with a multichannel scaler. For each mass spectrum, the ion arrival time resolution and accumulation time were 4 ns and 2 minutes (3600 sweeps), respectively.

Computational. The optimized geometries, harmonic vibrational frequencies, and infrared intensities of neutral H_4P_2O isomers and their cations are obtained by the hybrid density functional B3LYP/cc-pVTZ calculations.[10-13] Their energies are further refined utilizing coupled cluster[14-17] CCSD(T)/cc-pVDZ, CCSD(T)/cc-pVTZ, and CCSD(T)/cc-pVQZ, which are then extrapolated to completed basis set limits,[18] CCSD(T)/CBS, with B3LYP/cc-pVTZ zero-point energy corrections. The adiabatic ionization energies are computed by taking the difference between the ionic and the neutral states of similar conformation. The Gaussian 16 program[19] was used in the electronic structure calculations. The Cartesian coordinates, harmonic vibrational frequencies, and infrared intensities of the computed structures are listed in Tables S5 and S6.

Infrared Spectroscopy

Fourier transform infrared (FTIR) spectra of the phosphine−carbon dioxide ices were collected in situ at 5 K before, during, and after irradiation. The FTIR spectra of PH_3−CO_2 ice mixture (PH_3:CO_2, 1:10) are dominated by the fundamental vibrational modes of CO_2 (ν_3, 2349 cm^{-1}),[20] and PH_3 (ν_2, 986 cm^{-1}; ν_4, 1107 cm^{-1}),[8] along with combination bands of both reactants (Fig. S1, Table S3). After irradiation, new absorption features emerged at 2140 cm^{-1}, 2283 cm^{-1}, and 2460 cm^{-1}, which are assigned to the C≡O stretching of carbon monoxide (CO),[21] the PH_2 antisymmetric stretching (ν_1) of diphosphine (H_2PPH_2),[22] and the P−H stretching of other newly formed phosphorus-containing products,[23] respectively. Additionally, hydroxyphosphine (PH_2OH) produced via the reaction of PH_3 and atomic oxygen exhibits an absorption at 2279 cm^{-1} (ν_7) in an argon matrix,[24] suggesting that the observed 2283 cm^{-1} band might also be attributed to hydroxyphosphine. However, due to overlapping absorptions from functional groups in complex organics produced during irradiation and the limited sensitivity of our FTIR setup, infrared

spectroscopy alone is insufficient to unambiguously identify individual H_4P_2O isomers such as **1** and **2**, indicating that a more sensitive, isomer-specific analytical technique is required for the identification of reaction products.[25]

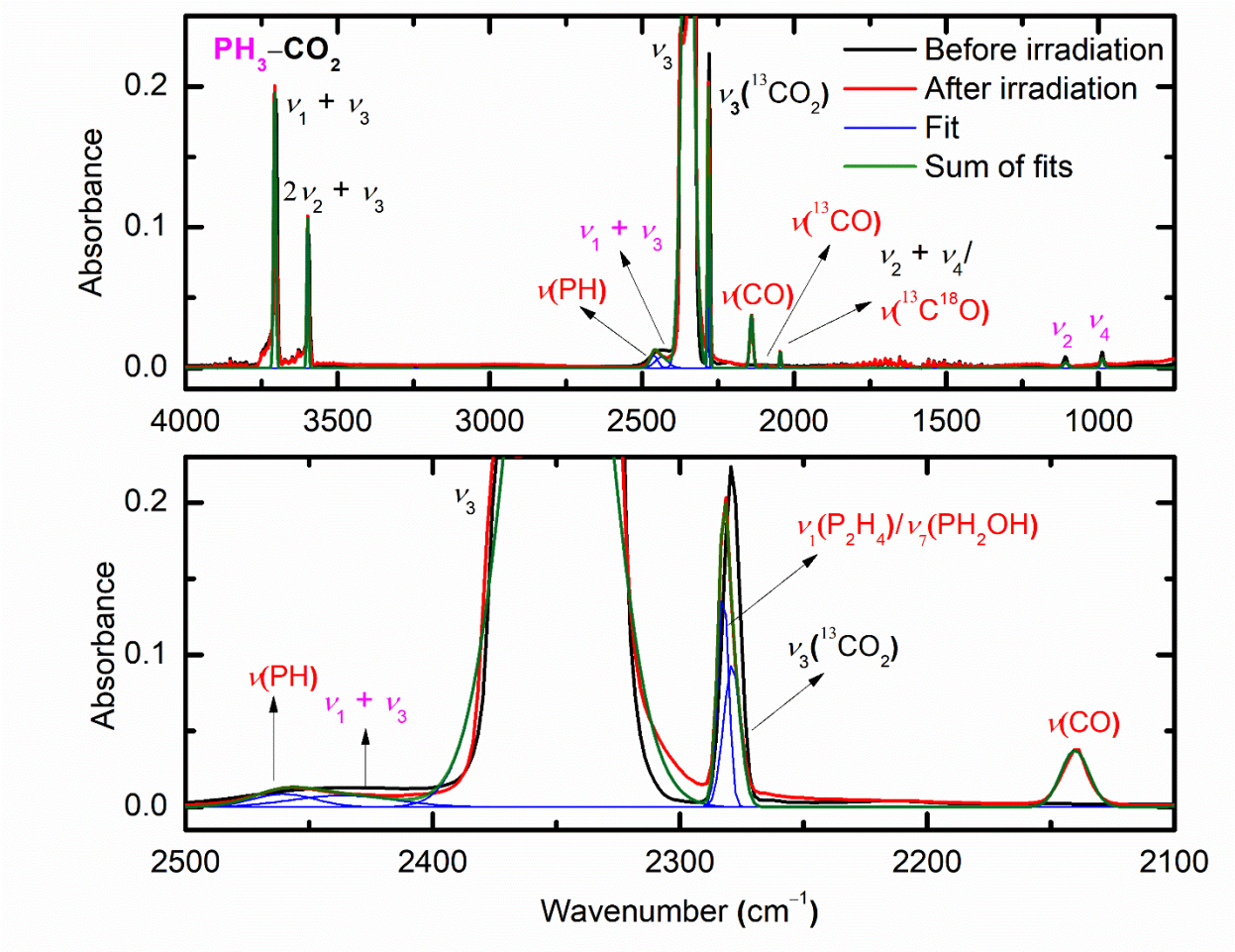

Figure S1. Infrared spectra (baseline corrected) of the PH_3–CO_2 ice collected before and after electron irradiation at 5 K (Top). The bottom panel shows a magnified view of the 2500–2100 cm^{-1} region with Gaussian deconvolution. The assignments of the absorptions of PH_3, CO_2, and new absorptions after irradiation are indicated in magenta, black, and red, respectively. Detailed assignments are provided in Table S3.

Table S1. Error analysis of adiabatic ionization energies (IEs) and relative energies (ΔE) of H_4P_2O isomers **1**−**3**, computed at the CCSD(T)/CBS//B3LYP/cc-pVTZ level including the zero-point vibrational energy (ZPVE) corrections. The IE ranges have been corrected for the thermal and Stark effect by −0.03 eV and combined error bounds of −0.03/+0.06 eV (Table S2).

Isomers	Structure	ΔE (kJ mol^{-1})	Computed IE (eV)	Corrected IE ranges (eV)
1a		25	9.15	9.09–9.18
1b	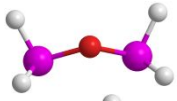	31	9.07	9.01–9.10
2a	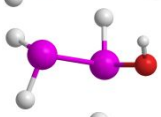	1	8.54	8.48–8.57
2b	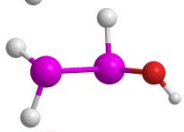	3	8.53	8.47–8.56
3	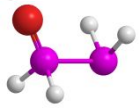	0	9.67	9.61–9.70

Table S2. Error analysis of adiabatic ionization energies (IEs) of 19 compounds, calculated at the CCSD(T)/CBS//B3LYP/cc-pVTZ level of theory including the zero-point vibrational energy corrections.

Molecules	Experimental IE (eV)	Computed IE (eV)	IE difference to lower bound (eV)	IE difference to upper bound (eV)
Hydrogen cyanide (HCN)	13.60 ± 0.01[26]	13.57	0.01	0.04
Methinophosphide (HCP)	10.79 ± 0.01[27]	10.76	0.02	0.04
Phosphine (PH_3)	9.869 ± 0.002[26]	9.82	0.047	0.051
Formaldehyde (H_2CO)	10.88 ± 0.01[26]	10.89	−0.02	0.00
Ketene (H_2CCO)	9.617 ± 0.003[26]	9.58	0.034	0.040
Acetonitrile (CH_3CN)	12.20 ± 0.01[26]	12.20	−0.01	0.01
Methanol (CH_3OH)	10.84 ± 0.01[26]	10.86	−0.03	−0.01
Acetaldehyde (CH_3CHO)	10.229 ± 0.0007[26]	10.24	−0.0117	−0.0103
Acetic acid (CH_3COOH)	10.65 ± 0.02[26]	10.65	−0.02	0.02
Vinylacetylene ($HCCCHCH_2$)	9.58 ± 0.02[26]	9.59	−0.03	0.01
Methylenecyclopropene (*c*-CH_2CCHCH)	8.15 ± 0.03[28]	8.11	0.01	0.07
1,2,3-Butatriene (H_2CCCCH_2)	9.15 ± 0.02[29]	9.14	−0.01	0.03
N-methyl formamide (CH_3NHCHO)	9.83 ± 0.04[26]	9.80	−0.01	0.07
Acetamide ($CH_3C(O)NH_2$)	9.77 ± 0.02[30]	9.74	0.01	0.05
Acetone ($CH_3C(O)CH_3$)	9.703 ± 0.006[26]	9.71	−0.013	−0.001
Propanal (CH_3CH_2CHO)	9.96 ± 0.01[26]	9.97	−0.02	0.00
Propylene oxide (*c*-CH_3CHOCH_2)	10.22 ± 0.02[26]	10.24	−0.04	0.00
2-Propen-1-ol (CH_2CHCH_2OH)	9.67 ± 0.03[26]	9.65	−0.01	0.05
(*E*)-1-Propenol ($CH_3CHCHOH$)	8.64 ± 0.02[31]	8.64	−0.02	0.02
			Average −0.01 ± 0.02	Average +0.03 ± 0.03
			Combined error limits −0.03 – +0.06	

Table S3. Observed absorption peaks of PH_3–CO_2 ice before and after irradiation at 5 K.

Pristine ice, absorptions before irradiation (cm^{-1})	
PH_3	Assignment[8]
3426	$\nu_1 + \nu_4$
2436	$\nu_1 + \nu_3$
2045	$\nu_2 + \nu_4$
1107	ν_4
986	ν_2
CO_2	Assignment[20]
3707	$\nu_1 + \nu_3$
3599	$2\nu_2 + \nu_3$
2349	ν_3
2279	ν_3 ($^{13}CO_2$)
1383, 1277	$2\nu_2$
673, 656	ν_2
New absorptions after irradiation (cm^{-1})	Assignment[21-24]
2460	ν(PH)
2283	$\nu_1(P_2H_4)$/$\nu_7(PH_2OH)$
2140	ν(CO)
2093	$\nu(^{13}CO)$
2046	$\nu(^{13}C^{18}O)$

Table S4. Generation parameters of vacuum ultraviolet (VUV) photons via the four-wave mixing method. The VUV photon energy uncertainty is less than 0.001 eV.

VUV photon energy (eV) $(2\omega_1 - \omega_2)$	Nonlinear medium	Wavelength for ω_1 (nm)	Dye for ω_1	Wavelength for ω_2 (nm)	Dye for ω_2
10.86	Krypton	202.316	Rhodamine 610 and 640	890	LDS 867
9.60	Krypton	202.316	Rhodamine 610 and 640	466.7	Coumarin 480
8.77	Xenon	249.628	Coumarin503	1064	–
8.11	Xenon	249.628	Coumarin503	679.9	LDS 698

Table S5. B3LYP/cc-pVTZ optimized cartesian coordinates (Å) on the adiabatic singlet and doublet ground state potential energy surface of H_4P_2O and $H_4P_2O^+$ isomers, respectively.

Atom	X	Y	Z	Atom	X	Y	Z
1a				**1a$^+$**			
O	-0.000847	0.658100	-0.071729	O	0.000000	0.000000	0.422188
H	-2.299943	0.902824	-0.101116	H	0.998756	2.082916	0.775609
H	-1.596372	-0.666776	-1.231081	H	0.680060	1.508388	-1.319864
P	1.511077	-0.027656	0.009616	P	0.000000	-1.556709	-0.076300
H	1.304197	-0.982120	1.057314	H	-0.998756	-2.082916	0.775609
H	1.384943	-1.046124	-0.990272	H	-0.680060	-1.508388	-1.319864
P	-1.430147	-0.203851	0.112983	P	0.000000	1.556709	-0.076300
1b				**1b$^+$**			
O	0.000000	0.000000	0.601560	O	0.026510	0.357757	-0.173147
H	-1.025875	2.100100	0.521395	H	1.786319	-1.174632	-0.744897
H	1.025875	2.100100	0.521395	H	2.250867	0.996702	-0.429299
P	0.000000	-1.454873	-0.229935	P	-1.562314	-0.088588	0.137779
H	1.025875	-2.100100	0.521395	H	-2.145767	1.009419	-0.535666
H	-1.025875	-2.100100	0.521395	H	-1.720247	-1.075503	-0.869725
P	0.000000	1.454873	-0.229935	P	1.536763	-0.085948	0.126539
2a				**2a$^+$**			
O	1.623706	-0.714829	-0.047843	O	1.586898	-0.706506	0.017904
H	1.377004	-1.355514	0.628746	H	2.460764	-0.573993	0.417200
H	0.616250	1.006882	1.274649	H	0.871509	1.438618	0.922091
P	-1.400317	-0.285766	0.058376	P	-1.440860	-0.217086	0.142855
H	-2.005892	0.913714	0.521993	H	-2.037552	0.949753	-0.404061
H	-1.783128	-0.076922	-1.293349	H	-1.468307	-0.998690	-1.040812
P	0.654058	0.634464	-0.108328	P	0.606087	0.539510	-0.145365
2b				**2b$^+$**			
O	1.579089	-0.737774	0.147772	O	-1.727077	0.565494	0.168152
H	2.207346	-0.838400	-0.572903	H	-1.844905	1.311998	-0.439357
H	0.595073	1.094749	1.208780	H	-0.825120	-1.440865	0.875969
P	-1.413157	-0.293263	0.073062	P	1.461386	0.220502	0.142101
H	-2.007519	0.959998	0.393573	H	2.047847	-0.968775	-0.366766
H	-1.755950	-0.192737	-1.303981	H	1.560946	0.986963	-1.047448
P	0.635046	0.618501	-0.133572	P	-0.602863	-0.514720	-0.166609

3				**3^+**			
O	1.455916	1.100578	0.000000	O	1.485153	0.620729	0.000000
H	-0.749652	1.303308	1.090671	H	-0.550438	1.526500	1.139247
H	-0.749652	1.303308	-1.090671	H	-0.550438	1.526500	-1.139247
P	-0.702320	-1.323209	0.000000	P	-0.724089	-1.215733	0.000000
H	0.193384	-1.693370	-1.037891	H	0.040495	-1.700699	-1.087807
H	0.193384	-1.693370	1.037891	H	0.040495	-1.700699	1.087807
P	0.000000	0.788243	0.000000	P	0.000000	0.907904	0.000000

Table S6. B3LYP/cc-pVTZ vibrational frequencies (cm^{-1}) and infrared intensities (km mol^{-1}) on the adiabatic singlet and doublet ground state potential energy surface of H_4P_2O and $H_4P_2O^+$ isomers, respectively.

Normal modes	Frequency(cm^{-1})	IR Intensity	Frequency(cm^{-1})	IR Intensity
	1a		**1a$^+$**	
*v*1	83.2396	4.7777	140.9948	10.0117
*v*2	180.0026	0.3611	179.658	318.5693
*v*3	217.4535	1.004	209.2393	647.7471
*v*4	618.2097	18.3006	224.8878	2.3493
*v*5	848.0701	320.3074	564.8847	7.703
*v*6	909.131	13.5064	855.9694	2.5524
*v*7	918.1302	24.9224	876.8588	5.6808
*v*8	971.1136	65.5064	891.7221	32.4677
*v*9	1004.16	37.7392	1036.544	21.1839
*v*10	1115.5607	16.1548	1076.7336	278.4215
*v*11	1133.0036	19.8721	1091.2845	0.0137
*v*12	2295.3981	64.3516	2382.4378	4.4431
*v*13	2303.9557	103.3749	2384.1402	1.8942
*v*14	2309.3374	123.1886	2433.0888	2.4911
*v*15	2360.7068	94.5733	2433.879	0.5064
	1b		**1b$^+$**	
*v*1	62.1022	5.0874	115.0203	36.1112
*v*2	80.469	0	174.8858	682.2058
*v*3	229.2388	2.3769	216.2174	58.9371
*v*4	612.2903	13.6664	235.3642	29.6689
*v*5	794.1718	299.8359	569.7157	64.2939
*v*6	895.5129	12.9291	855.0951	12.8158
*v*7	926.5498	0	881.0245	19.0399
*v*8	996.2265	41.788	900.4438	23.1448
*v*9	1028.0897	119.3783	1030.8306	7.4446
*v*10	1132.053	29.6605	1078.4549	230.2703
*v*11	1141.8164	11.7928	1107.9962	35.442
*v*12	2337.6955	143.6224	2386.0732	4.0812
*v*13	2343.5171	0	2387.0021	3.0965
*v*14	2344.0355	65.4774	2433.8541	2.3577

*v*15	2344.6308	207.0843	2452.0657	1.5287
	2a		**2a**$^{+}$	
*v*1	166.1966	2.9576	138.5534	12.487
*v*2	214.0899	11.4747	190.9216	63.8755
*v*3	372.8361	134.5011	256.6387	89.8911
*v*4	417.548	2.9066	422.1248	8.3404
*v*5	641.7367	13.9918	506.8152	36.8077
*v*6	685.0265	4.2644	718.1465	55.0298
*v*7	787.9719	153.5414	785.6744	9.6746
*v*8	879.5943	4.2199	873.8407	117.6802
*v*9	935.4593	39.308	912.8515	59.5209
*v*10	1066.4844	43.1846	1035.5244	45.7489
*v*11	1111.5411	7.3801	1067.9043	14.5199
*v*12	2289.0531	91.2317	2376.1432	2.1948
*v*13	2379.0942	38.0423	2396.5105	0.5297
*v*14	2389.6932	57.7579	2417.3763	0.1466
*v*15	3786.702	41.2315	3744.047	407.7667
	2b		**2b**$^{+}$	
*v*1	137.1597	1.6925	145.7471	0.3742
*v*2	188.3492	25.2531	220.3773	4.1215
*v*3	264.465	31.2443	333.9447	41.9516
*v*4	424.7886	10.4709	402.2567	0.466
*v*5	638.6987	17.4627	534.3701	102.4571
*v*6	702.1402	17.3747	695.1772	17.1247
*v*7	777.5635	124.0475	785.8395	17.6208
*v*8	874.2319	13.3377	892.947	191.0556
*v*9	950.2374	2.5813	950.8234	48.97
*v*10	1098.7022	7.4699	1041.256	41.5459
*v*11	1115.9587	95.6406	1069.7557	28.4105
*v*12	2339.2167	48.8863	2394.7738	0.3634
*v*13	2366.2352	45.8263	2415.4415	0.2789
*v*14	2376.1386	80.8284	2439.0792	1.3615
*v*15	3841.2068	121.9912	3748.2243	314.2121
	3		**3**$^{+}$	
*v*1	170.1943	8.7254	175.9351	12.0617
*v*2	237.5717	19.5234	194.2245	27.105
*v*3	425.8362	16.1334	399.5663	6.5611

*v*4	489.0039	17.8847	511.9291	5.5098
*v*5	695.1088	28.068	554.8904	100.0013
*v*6	792.397	2.2238	728.4067	0.7224
*v*7	922.4312	2.6681	803.8178	4.0821
*v*8	1014.0582	92.1865	881.7492	19.886
*v*9	1097.1909	0.629	1066.1051	13.7471
*v*10	1116.8326	48.0638	1073.3865	33.8256
*v*11	1234.7438	137.4456	1129.6938	76.4992
*v*12	2359.1367	65.9513	2417.6831	7.2271
*v*13	2363.7753	78.8721	2441.6003	1.2437
*v*14	2392.1397	26.2769	2445.7026	3.9534
*v*15	2402.6816	44.1269	2477.626	1.0559

References

(1) Jones, B. M.; Kaiser, R. I. Application of reflectron time-of-flight mass spectroscopy in the analysis of astrophysically relevant ices exposed to ionization radiation: Methane (CH_4) and D4-methane (CD_4) as a case study. *J. Phys. Chem. Lett.* **2013**, *4*, 1965-1971.

(2) Turner, A. M.; Bergantini, A.; Abplanalp, M. J.; Zhu, C.; Góbi, S.; Sun, B.-J.; Chao, K.-H.; Chang, A. H. H.; Meinert, C.; Kaiser, R. I. An interstellar synthesis of phosphorus oxoacids. *Nat. Commun.* **2018**, *9*, 3851.

(3) Zhu, C.; Frigge, R.; Turner, A. M.; Kaiser, R. I.; Sun, B.-J.; Chen, S.-Y.; Chang, A. H. First identification of unstable phosphino formic acid (H_2PCOOH). *ChemComm.* **2018**, *54*, 5716-5719.

(4) Kaiser, R. I.; Roessler, K. Theoretical and laboratory studies on the interaction of cosmic-ray particles with interstellar ices. I. Synthesis of polycyclic aromatic hydrocarbons by a cosmic-ray-induced multicenter mechanism. *Astrophys. J.* **1997**, *475*, 144.

(5) Drouin, D.; Couture, A. R.; Joly, D.; Tastet, X.; Aimez, V.; Gauvin, R. CASINO V2.42 - A fast and easy-to-use modeling tool for scanning electron microscopy and microanalysis users. *Scanning* **2007**, *29*, 92-101.

(6) Yeghikyan, A. G. Irradiation of dust in molecular clouds. II. Doses produced by cosmic rays. *Astrophysics* **2011**, *54*, 87-99.

(7) Francia, M. D.; Nixon, E. R. Infrared study of solid phosphine. *J. Chem. Phys.* **1973**, *58*, 1061-1065.

(8) Turner, A. M.; Abplanalp, M. J.; Chen, S. Y.; Chen, Y. T.; Chang, A. H. H.; Kaiser, R. I. A photoionization mass spectroscopic study on the formation of phosphanes in low temperature phosphine ices. *Phys. Chem. Chem. Phys.* **2015**, *17*, 27281-27291.

(9) Satorre, M. Á.; Domingo, M.; Millán, C.; Luna, R.; Vilaplana, R.; Santonja, C. Density of CH_4, N_2 and CO_2 ices at different temperatures of deposition. *Planet. Space Sci.* **2008**, *56*, 1748-1752.

(10) Becke, A. D. Density-functional thermochemistry. I. The effect of the exchange-only gradient correction. *J. Chem. Phys.* **1992**, *96*, 2155-2160.

(11) Becke, A. D. Density-Functional Thermochemistry. II. The Effect of the Perdew–Wang Generalized-Gradient Correlation Correction. *J. Chem. Phys.* **1992**, *97*, 9173-9177.

(12) Becke, A. D. Density-functional thermochemistry. III. The role of exact exchange. *J. Chem. Phys.* **1993**, *98*, 5648-5652.

(13) Lee, C.; Yang, W.; Parr, R. G. Development of the Colle-Salvetti correlation-energy formula into a functional of the electron density. *Phys. Rev. B* **1988**, *37*, 785-789.

(14) Purvis III, G. D.; Bartlett, R. J. A Full Coupled-Cluster Singles and Doubles Model: The Inclusion of Disconnected Triples. *J. Chem. Phys.* **1982**, *76*, 1910-1918.

(15) Hampel, C.; Peterson, K. A.; Werner, H.-J. A Comparison of the Efficiency and Accuracy of the Quadratic Configuration Interaction (QCISD), Coupled Cluster (CCSD), and Brueckner Coupled Cluster (BCCD) Methods. *Chem. Phys. Lett.* **1992**, *190*, 1-12.

(16) Knowles, P. J.; Hampel, C.; Werner, H. J. Coupled cluster theory for high spin, open shell reference wave functions. *J. Chem. Phys.* **1993**, *99*, 5219-5227.

(17) Deegan, M. J.; Knowles, P. J. Perturbative Corrections to Account for Triple Excitations in Closed and Open Shell Coupled Cluster Theories. *Chem. Phys. Lett.* **1994**, *227*, 321-326.

(18) Peterson, K. A.; Woon, D. E.; Jr., T. H. D. Benchmark calculations with correlated molecular wave functions. IV. The classical barrier height of the $H+H_2 \rightarrow H_2+H$ reaction. *J. Chem. Phys.* **1994**, *100*, 7410-7415.

(19) M. J. Frisch, G. W. T., H. B. Schlegel, G. E. Scuseria, M. A. Robb, J. R. Cheeseman, G. Scalmani, V. Barone, G. A. Petersson, H. Nakatsuji, X. Li, M. Caricato, A. V. Marenich, J. Bloino, B. G. Janesko, R. Gomperts, B. Mennucci, H. P. Hratchian, J. V. Ortiz, A. F. Izmaylov, J. L. Sonnenberg, D. Williams-Young, F. Ding, F. Lipparini, F. Egidi, J. Goings, B. Peng, A. Petrone, T. Henderson, D. Ranasinghe, V. G. Zakrzewski, J. Gao, N. Rega, G. Zheng, W. Liang, M. Hada, M. Ehara, K. Toyota, R. Fukuda, J. Hasegawa, M. Ishida, T. Nakajima, Y. Honda, O. Kitao, H. Nakai, T. Vreven, K. Throssell, J. A. Montgomery, Jr., J. E. Peralta, F. Ogliaro, M. J. Bearpark, J. J. Heyd, E. N. Brothers, K. N. Kudin, V. N. Staroverov, T. A. Keith, R. Kobayashi, J. Normand, K. Raghavachari, A. P. Rendell, J. C. Burant, S. S. Iyengar, J. Tomasi, M. Cossi, J. M. Millam, M. Klene, C. Adamo, R. Cammi, J. W. Ochterski, R. L. Martin, K. Morokuma, O. Farkas, J. B. Foresman, D. J. Fox; Gaussian Inc. Wallingford, CT: 2016.

(20) Bouilloud, M.; Fray, N.; Benilan, Y.; Cottin, H.; Gazeau, M. C.; Jolly, A. Bibliographic review and new measurements of the infrared band strengths of pure molecules at 25 K: H_2O, CO_2, CO, CH_4, NH_3, CH_3OH, HCOOH and H_2CO. *Mon. Not. R. Astron. Soc.* **2015**, *451*, 2145-2160.

(21) Wang, J.; Turner, A. M.; Marks, J. H.; Zhang, C.; Kleimeier, N. F.; Bergantini, A.; Singh, S. K.; Fortenberry, R. C.; Kaiser, R. I. Preparation of acetylenediol (HOCCOH) and glyoxal (HCOCHO) in interstellar analog ices of carbon monoxide and water. *Astrophys. J.* **2024**, *967*, 79.

(22) Durig, J. R.; Shen, Z.; Zhao, W. Conformational stability, structural parameters, and vibrational frequencies from ab initio calculations for biphosphine. *J. Mol. Struct.* **1996**, *375*, 95-104.

(23) Socrates, G. *Infrared and raman characteristic group frequencies: Tables and charts*; 3rd ed.; John Wiley & Sons, Ltd.: New York, 2004.

(24) Withnall, R.; Andrews, L. Infrared spectra of oxygen atom-phosphine reaction products trapped in solid argon. *J. Phys. Chem.* **1988**, *92*, 4610-4619.

(25) Turner, A. M.; Kaiser, R. I. Exploiting photoionization reflectron time-of-flight mass spectrometry to explore molecular mass growth processes to complex organic molecules in interstellar and solar system ice analogs. *Acc. Chem. Res.* **2020**, *53*, 2791-2805.

(26) P. J. Linstrom; Mallard, W. G. NIST Chemistry webBook, NIST Standard Reference Database Number 69, **2013**, http://webbook.nist.gov/.

(27) Frost, D. C.; Lee, S. T.; McDowell, C. A. The photoelectron spectrum of HCP and comments on the first photoelectron band of HCN. *Chem. Phys. Lett.* **1973**, *23*, 472-475.

(28) Staley, S. W.; Norden, T. D. Structure and energetics of $C_4H_4^{\cdot+}$ in the gas phase. Photoelectron spectrum of methylenecyclopropene. *J. Am. Chem. Soc.* **1989**, *111*, 445-449.

(29) Brogli, F.; Heilbronner, E.; Kloster-Jensen, E.; Schmelzer, A.; Manocha, A. S.; Pople, J. A.; Radom, L. The photoelectron spectrum of butatriene. *Chem. Phys.* **1974**, *4*, 107-119.

(30) Watanabe, K.; Nakayama, T.; Mottl, J. Ionization potentials of some molecules. *J. Quant. Spectrosc. Radiat. Transfer* **1962**, *2*, 369-382.

(31) Tureček, F. (E)- and (Z)-prop-1-en-1-ol: gas-phase generation and determination of heats of formation by mass spectrometry. *J. Chem. Soc., Chem. Commun.* **1984**, 1374-1375.